Evaluating the On-Demand Mobile Charging in Wireless Sensor Networks

Liang He, *Member, IEEE*, Linghe Kong, *Member, IEEE*, Yu Gu, *Member, IEEE*,
Jianping Pan, *Senior Member, IEEE*, and Ting Zhu, *Member, IEEE*

Abstract—Recently, adopting mobile energy chargers to replenish the energy supply of sensor nodes in wireless sensor networks has gained increasing attention from the research community. Different from energy harvesting systems, the utilization of mobile energy chargers is able to provide more reliable energy supply than the dynamic energy harvested from the surrounding environment. While pioneering works on the mobile recharging problem mainly focus on the optimal *offline* path planning for the mobile chargers, in this work, we aim to lay the theoretical foundation for the *on-demand* mobile charging (DMC) problem, where individual sensor nodes request charging from the mobile charger when their energy runs low. Specifically, in this work, we analyze the on-demand mobile charging problem using a simple but efficient *Nearest-Job-Next with Preemption* (NJNP) discipline for the mobile charger, and provide analytical results on the system throughput and charging latency from the perspectives of the mobile charger and individual sensor nodes, respectively. To demonstrate how the actual system design can benefit from our analytical results, we present two examples on determining the essential system parameters such as the optimal remaining energy level for individual sensor nodes to send out their recharging requests and the minimal energy capacity required for the mobile charger. Through extensive simulation with real-world system settings, we verify that our analytical results match the simulation results well and the system designs based on our analysis are effective.

Index Terms—Wireless ad hoc sensor networks, mobile charger, on-demand energy replenishment

✦

1 INTRODUCTION

FOR real-world sensor network applications, sensor nodes are usually powered by on-board batteries or super-capacitors [1], [2], [3], [4]. This limited energy supply makes energy the most precious resource in the system, and thus its efficient usage is highly demanded.

Recently, research efforts begin to explore the concept of mobile energy chargers to replenish the energy supply of individual sensor nodes to improve the system sustainability [5], [6], [7], [8]. Prototypes of such mobile charging are implemented in [9], [10]. For most existing research, researchers have mainly focused on the *offline* scenarios [5], [7], [8], [11], [12], in which the charging of individual nodes is carried out in a *periodic* and *deterministic* manner. However, due to the close interaction with the surrounding environment, the energy consumption profiles of the nodes in the network demonstrate high diversity. Furthermore, for sensor nodes integrated with energy-harvesting modules, the amount of the harvested energy also fluctuates greatly [1], [2]. The uncertainty in both the energy demand and

supply indicates that existing periodic charging solutions may suffer from non-negligible performance degradation.

Observing the limitation of existing solutions, in this paper we investigate the on-demand energy replenishment in wireless sensor networks, and aim to lay the theoretical foundation for such an on-demand charging process. Specifically, we are interested in answering questions such as *how the mobile charger should schedule and carry out the charging of individual nodes without a priori knowledge on the demands raised in the near future, and what the achievable performance is*. We analytically investigate a simple but efficient *Nearest-Job-Next with Preemption* (NJNP) discipline for the on-demand mobile charging (DMC) problem, which schedules the charging of individual nodes according to their spatial and temporal properties. We prove that the asymptotic performance of NJNP is within constant factors of the optimal solutions. We also present two examples on how these analyses guide the implementation of NJNP in practice. Specifically, our contributions in this paper include:

- We mathematically formulate the DMC problem in wireless sensor networks, and theoretically establish the charging performance with the *Nearest-Job-Next with Preemption* discipline. These analytical results not only shed light on the performance of NJNP, but also provide useful guidances for the design of more sophisticated charging schemes. To the best of our knowledge, this is the first in-depth work to analytically evaluate the performance of the DMC in sensor networks.

- We present four theorems that demonstrate the asymptotic performance of NJNP is within constant factors of the optimal results with respect to the

- *L. He is with the University of Michigan at Ann Arbor, 2260 Hayward St. Ann Arbor, MI 48109. E-mail: lianghe.umich@gmail.com.*
- *L. Kong is with the Shanghai Jiaotong University, China. E-mail: linghe.kong@sjtu.edu.cn.*
- *Y. Gu is with the IBM Research, Austin, TX 78758. E-mail: jasongu@sutd.edu.sg.*
- *J. Pan is with the University of Victoria, Victoria, BC, Canada. E-mail: pan@uvic.ca.*
- *T. Zhu is with the University of Maryland, Baltimore County, MD 21250. E-mail: tzhu@binghamton.edu.*

Fig. 1. Lab settings for WISP-based charging.

Fig. 2. Measurements results on received power.

system throughput and charging latency of individual nodes, under both light and heavy charging demands in the system.

- With these analytical results on NJNP, we use two examples to demonstrate how our results can guide the implementation of NJNP for real-world sensor networks. Specifically, we discuss how to determine key system parameters such as the optimal remaining energy level for individual nodes to send out their recharging requests and the minimal energy capacity required for the mobile charger.

Here we emphasize that while we demonstrate the performance of NJNP is promising, we are not suggesting that NJNP is the *best* discipline and should be directly adopted. Instead, the purpose of this work is to establish a solid foundation for understanding the performance of NJNP-based on-demand charging processes and provide guidances on designing more advanced charging schemes and determining optimal system parameters. Furthermore, with the theoretically proved performance, NJNP also serves as a perfect benchmark to evaluate more advanced schemes.

2 PRELIMINARIES

2.1 Charging Technologies

With the advance of energy transferring technologies, the time to replenish the energy supply of sensor nodes has been dramatically reduced [13]. In our previous work [2], an energy sharing system with capacitor-array powered MicaZ motes is implemented, in which the energy in the system is transferred from energy-rich to energy-hungry nodes with a high efficiency of around 90 percent. Furthermore, from our empirical results in [1], the time to charge a 10 F super-capacitor to a voltage of 2.5 V is normally in the order of tens of seconds. This continuously shortened charging time makes adopting mobile chargers to replenish the energy supply of individual nodes a promising approach to achieving the stable and sustainable network operation.

Most existing research efforts adopt the contact-free wireless charging technology for the mobile charger to replenish node energy [5], [9], [10]. Although the wireless charging technology has advanced, it still suffers from a low charging efficiency. Experiment measurements reported in [9] show that the efficiency of the PowerCast wireless charging solution [14] is only around 1.5 percent even with a short distance of 10 cm. We also conducted wireless charging experiments with the wireless identification and sensing platform (WISP) [15] as shown in Fig. 1. The resultant received power values with regard to the distance between the transmitter (i.e., charger) and the receiver (i.e., WISP nodes) are shown in Fig. 2. We can see that the
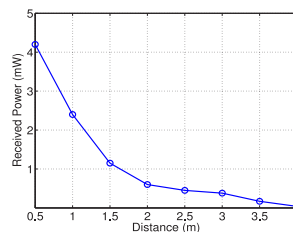
received power at the receiver is only about 1–5 mW with a distance of a few meters. With a transmitter transmitting power of 1 W, this indicates a charging efficiency of no higher than 0.5 percent.

On the other hand, the contact-based energy transferring technologies can achieve a much higher efficiency. For example, it is reported in [16] that the 2-D waveguide power transmission technology can achieve an energy efficiency of 87.7 percent. However, the limitation of the contact-based charging technologies is the requirement on the docking between the charger and sensor nodes, which may impose high accuracy requirement on the localization and navigation of the mobile charger. Sophisticated designs on the docking between a mobile device and a static device exist in the literature. For example, Silverman et al. proposed a sensor-based docking mechanism in [17]. The contact-based charging technology is also adopted in *off-the-shelf* products such as iRobot Roomba [18] and Nokia wireless charging plate for smartphones [19].

Observing the high efficiency of the contact-based charging technologies and the advancement of docking mechanisms, we in this work focus on the scenario where the mobile charger replenishes the energy supply of nodes with contact-based charging technologies. However, our modeling and analysis on the mobile charging process are not restricted to certain specific charging technologies. In fact, it is applicable to all mobile charging scenarios where the charging distance is relatively short when compared with the charger travel distance to rendezvous with the sensor node.

2.2 Problem Statement

For the DMC problem, we consider wireless sensor networks where nodes are randomly deployed to monitor the surrounding environment. Nodes actively monitor their residual energy [9], which can be realized either by the nodes themselves, or by adopting specialized companion modules to improve the accuracy [2]. Nodes send out charging request to mobile chargers when their energy level falls below a certain threshold. Such lightweight communications can be accomplished by adopting the *state-of-the-art* protocols for tracking and communicating with the mobile charger [20]. The request delivery time is assumed to be negligible when compared with the travel time and charging time [3], and its impact on the mobile charging process will be explored through simulation in Section 5. At the mobile charger, it maintains a service pool to store the received requests, and serves them according to its charging discipline. By serving a request, we mean the mobile charger moves to the corresponding node and fully charges it. For the ease of presentation, the term *serve a charging request* and *replenish the energy supply of the corresponding node* are
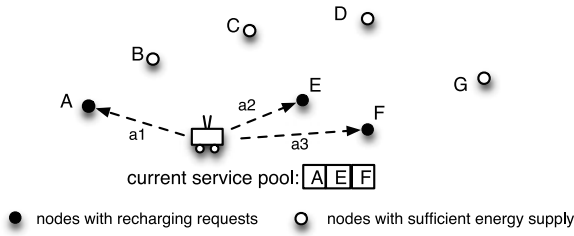
Fig. 3. On-demand charging of nodes: a_1, a_2, and a_3 represent the corresponding distances to requesting nodes.

used interchangeably. An example of the DMC process is presented in Fig. 3, where three charging requests from nodes A, E, and F have been received, and the charger needs to select one of them as the next node to charge.

Different from the offline charging scenario, the charging tasks in the on-demand scenario exhibit highly dynamic properties in both the *temporal* dimension, i.e., when a new charging request arrives, and the *spatial* dimension, i.e., where the new demand comes from (or the request is sent by which node). Such dynamic properties suggest that our design for the DMC problem should shift from the optimal *path planning* for the mobile charger as that in the offline scenario [5], to the design of efficient scheduling disciplines to select the next to-be-charged node, in terms of both the workloads of the charger and the charging latency of nodes.[1]

2.3 Nearest Job Next with Preemption

The simplest and most intuitive scheduling discipline is *First-Come-First-Serve* (FCFS), whose performance has been extensively studied by the queuing theory community [21]. However, FCFS schedules the incoming charging requests based on only their *temporal* property and could lead to the back-and-forth charger movement in the *spatial* dimension [9].

Observing the limitation of FCFS, in this work, we explore another discipline, *Nearest-Job-Next with Preemption*, which considers both the *spatial* and *temporal* properties of incoming requests, allowing the mobile charger to switch to a spatially closer target node if the new requesting node is of a shorter distance to the mobile charger. More specifically, under NJNP, *each charging completion of nodes and the arrival of new charging requests trigger the re-selection of the next to-be-charged node, and the mobile charger selects the spatially closest requesting node at that time as the next node to charge.* Clearly, with the contact-based charging technologies, the preemption of charging tasks can occur only before the mobile charger reaches the target node, after which the distance between them can be mathematically treated as zero.

3 ON-DEMAND CHARGING WITH NJNP

We investigate the DMC problem with NJNP in this section, which can be evaluated from two aspects.

- *Throughput*. From the view of the mobile charger, the *throughput* of the charging process, defined as the number of requests the mobile charger can serve
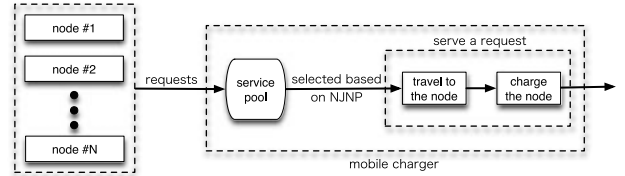
during a given time period, is the essential metric to evaluate the capability of the system in providing the charging service to individual nodes.
- *Charging latency*. On the other hand, the *charging latency* of the request, defined as the time since the request is sent by a node to the time it is fully charged, is what the nodes care the most.

In the following, we analytically investigate the charging process from these two aspects respectively.

For the mobile charger, the selection of requests from its service pool demonstrates a clear queuing behavior, which inspires us to adopt a queuing model to investigate and analyze the charging process: the mobile charger serves as the *server* and the charging requests sent by nodes are treated as *clients*. More specifically, an $M/G/1/NJNP$ queuing model is adopted, as shown in Fig. 4. The performance of the NJNP-based mobile charging process is analytically evaluated with the assistance of a few existing results from geometrical probability and first-order statistic. The soundness of this model in capturing the DMC problem is further verified in Section 5.

3.1 System Throughput with NJNP

To serve a request, the mobile charger needs to first move to the corresponding node and then charge it, and thus the time to serve each request consists of two parts: the travel time and the charging time.

For the charging time, we simplify the analysis by considering the worst-case charging time T_c, which is needed for the mobile charger to fully charge an energy-depleted node, and our analysis can be easily extended for more dynamic charging times, as will be explained in Section 3.1.1.

Due to the dynamics in both the charger's movement and the set of requesting nodes at random time instances, when the charger selects the next node to charge, its current location and that of the selected node can be viewed as two random locations in the deployment area. The distance between random locations in a specific shape is a well-studied topic in geometrical probability. Without loss of generality, we assume a unit square deployment area in this work, and the distance d between two random locations follows the distribution [22]

$$f_D(d) = \begin{cases} 2d(\pi - 4d + d^2) & d \in [0,1] \\ 2d[2\sin^{-1}(\frac{1}{d}) - 2\sin^{-1}\sqrt{1 - \frac{1}{d^2}} \\ \quad + 4\sqrt{d^2 - 1} - d^2 - 2] & d \in (1, \sqrt{2}] \\ 0 & \text{otherwise} \end{cases}, \quad (1)$$

where the second case differs from the first one because for d to be larger than 1, at least one of the two points must fall outside the inscribed circle of the square. In the case where

Fig. 4. Demonstration of the queuing model.

---

1. Note that we focus on the case where the charger energy capacity is enough for the charging process under consideration in the rest of the paper. We will show how the charging of the charger itself can be seamlessly incorporated into the charging process in Section 6.

the deployment field cannot be approximated by a square, we can substitute (1) with corresponding distance distributions for that field [23], which does not affect the following analysis.

With NJNP, the mobile charger always selects the nearest requesting node as the next to charge. Intuitively, the more nodes waiting to be charged, the more likely for the mobile charger to find a spatially closer node to charge. Thus we investigate the system throughput under NJNP in two steps: first focus on the case where the number of waiting requests is given, and then extend the analysis to a more general case.

3.1.1 Charging with a Given Number of Requests

Consider the case that l requests are waiting to be served when the mobile charger just accomplishes the service of the current request (or a new request is just received by the charger). With the current location of the mobile charger, we can approximately treat the distances from the l requesting nodes to the mobile charger as l independent and identically distributed (i.i.d.) random variables conforming to $f_D(d)$.[2] We will further verify this i.i.d. condition in Section 5. With the greedy NJNP scheme which always selecting the closest requesting node as the next target to charge, among these l distances (e.g., a_1, a_2, and a_3 in Fig. 3), the mobile charger selects the node (node E in Fig. 3) with the shortest distance (a_2 in Fig. 3) as the next charging target. Clearly, this is the *first-order statistic* [24], i.e., finding the smallest one of l i.i.d. variables. The distribution of the shortest distance to these l nodes can be calculated by

$$F_D(d, l) = \sum_{i=0}^{l-1} \binom{l}{i}(1 - F_D(d))^i F_D(d)^{l-i}$$
$$= 1 - (1 - F_D(d))^l. \tag{2}$$

where $F_D(d)$ is the cumulative distribution function (CDF) of $f_D(d)$ defined in (1), i.e., $F_D(d) = \int_0^d f_D(x)dx$, l is the number of pending requests, and d is the distance between the charger and the requesting sensor nodes.

Thus with a constant travel speed v, the time for the mobile charger to travel through this distance follows a distribution of

$$F_T(t, l) = F_D(vt, l)(0 \leq t \leq \sqrt{2}/v), \tag{3}$$

where v is the charger travel speed. The maximal possible travel time $\frac{\sqrt{2}}{v}$ happens when the mobile charger locates at one corner of the square area while the requesting node is located at the diagonal corner, and no preemption happens before the mobile charger arrives at that node. Denote the corresponding probability density function (PDF) as $f_T(t, l) = \partial F_T(t, l)/\partial t$.

2. In systems which require the coordinated operation among spatially closely located nodes, the requests of energy replenishment from these nodes may show certain correlation. Although this correlation may make our analysis deviate from the reality, it actually improves the performance of NJNP because requesting nodes will be more closely located, and thus our analytical results can be treated as performance lower bounds of NJNP.

Still let us consider the case that l requests are in the service pool and denote the distance between the mobile charger and the closest requesting node as d. Therefore, the time for the mobile charger to reach this closest requesting node is $t = \frac{d}{v}$. We discretize t into a sequence of short time slots with a duration of δ_t and define $z = \frac{t}{\delta_t}$, and thus at most one new arrival can occur during each time slot. For the first preemption to occur at the ith time slot ($1 \leq i \leq z - 1$), two conditions must hold

1) a new request has to be received during the ith slot, which happens with probability $\lambda \delta_t$, and λ is the aggregated arrival rate of charging requests at the mobile charger;
2) the node sending the new request has to be within distance $d - iv\delta_t$ to the mobile charger, which happens with probability $F_D(d - iv\delta_t)$.

Define $q_d(i) = \lambda \delta_t F_D(d - iv\delta_t)$, then the probability for a charging task with an initial travel distance d to be preempted is

$$q_d = 1 - \sum_{i=1}^{z-1}(1 - q_d(i)). \tag{4}$$

If the mobile charger arrives at a requesting node at the ith time slot ($1 \leq i \leq z - 1$), it indicates there exists a requesting node with a distance no longer than $v\delta_t$ from the mobile charger during the $(i-1)$th time slot. Let $p_d^l(i)$ and l_i be the probability that the charger arrives at the destination node at time slot i and the service pool size at time slot i respectively, we observe the following recursive relationship

$$p_d^l(i) = \prod_{j=1}^{i-1}\big(1 - p_d^l(j)\big) F_D(v\delta_t, l_{i-1}). \tag{5}$$

For the service pool sizes $\{l_0, l_1, \ldots, l_{i-1}\}$, because no departure of charging requests occurs between time 0 to time $i - 1$, the sequence of service pool sizes is non-decreasing

$$0 \leq l_1 - l_0 \leq l_2 - l_0 \leq \cdots \leq l_{i-1} - l_0 \leq X_j,$$

where X_j is the number of new charging requests arrived during this time. In a stable system, the number of new charging requests between two consecutive service completions is limited, and thus X_j is normally a small number. Furthermore, because we discretize the time into a sequence of short time slot δ_t, $F_D(v\delta_t, l)$ is a small positive value. Based on the above observations, we use $\beta = F_D(v\delta_t, l)$ to approximate $F_D(v\delta_t, l_i)$ in (5), and thus $p_d^l(i)$ can be calculated by considering another fact that $\sum_{i=1}^{z} p_d^l(i) = 1$. Specifically, we have

$$p_d^l(i) \approx \begin{cases} \prod_{j=1}^{i-1}(1 - p_d^l(j))\beta & 1 \leq i \leq z - 1 \\ 1 - \sum_{i=1}^{z-1} p_d^l(i) & i = z, \end{cases}$$

and the first and second case occur with probability q_d and $1 - q_d$ respectively. Thus the distribution of the travel time with service pool size l can be calculated as

$$f_{S'_l}(t) = \int_t^{\sqrt{2}/v} p_x^l(t/\delta_t) \cdot f_T(x, l)dx,$$

and with charging time T_c, the time to replenish the energy supply of a node follows the distribution of

$$f_{\mathcal{S}_l}(t) = f_{\mathcal{S}'_l}(t - T_c)(T_c \le t \le T_c + \sqrt{2}/v). \tag{6}$$

Note that when the charging time of a node is dynamic, we can empirically estimate the charging time profile $f_C(t)$ and adopt the convolution theorem to substitute (6) as $f_{\mathcal{S}_l}(t) \sim f_{\mathcal{S}'_l}(t) * f_C(t)$, where $*$ represents the convolution operation.

3.1.2 Charging in the General Case

So far all our analysis is based on the conditional service pool size l, and thus we need to investigate l to generalize our results. An *embedded discrete-time Markov chain* can be observed if we view the service pool size only at requests departure times, and thus the departure-time system size probabilities can be obtained with a Markov chain-based approach by defining [21]

$$\Pr\{X_j = i\} = a_i^j = \int_{T_c}^{\sqrt{2}/v + T_c} \frac{e^{-\lambda t}(\lambda t)^i}{i!} f_{\mathcal{S}_j}(t)dt. \tag{7}$$

where λ is the aggregated arrival rate of charging requests at the mobile charger.[3]

Denote the obtained departure-time system size probabilities as $\boldsymbol{\pi}$. While $\boldsymbol{\pi}$ in general is different from the probabilities of steady-state system size, for the $M/G/1$ queue, these two quantities have been proved to be asymptotically identical [21].

Applying $\boldsymbol{\pi}$ to (6), we can derive the general service time distribution of charging requests as

$$F_{\mathcal{S}}(t) = \pi_0 \int_0^t f_{\mathcal{S}_1}(x)dx + \sum_{l=1}^N \pi_l \int_0^t f_{\mathcal{S}_l}(x)dx, \tag{8}$$

where N is the number of nodes in the system and $f_{\mathcal{S}}(t) = \partial F_{\mathcal{S}}(t)/\partial t$. The first term on the right side of (8) accounts for the requests arrive at an empty service pool, and the second term corresponds to the requests that experience a busy system upon arrival.

The system throughput with NJNP, $\mathcal{H}_{njnp}$, follows

$$\Pr\{\mathcal{H}_{njnp} < h\} = 1 - F_{\mathcal{S}}(1/h), \tag{9}$$

and the expected system throughput with NJNP is

$$\mathrm{E}[\mathcal{H}_{njnp}] = \frac{1}{\int_{T_c}^{T_c + \sqrt{2}/v} t \cdot f_{\mathcal{S}}(t)dt}. \tag{10}$$

For any stable queuing system, a well-known result is its system utility ρ, defined as the ratio between the clients arrival rate and system service rate, should be smaller than 1. In our DMC problem, this condition takes the form of $\rho = \lambda \mathrm{E}[\mathcal{H}_{njnp}] < 1$.

3. Note that we do not require the homogeneous sub-processes from individual sensor node, as it has been known that the superposition of n sub-processes resembles a Poisson process whose arrival rate is the sum of all the sub-processes, especially when n is large [25], [26].

3.1.3 Optimality w.r.t. System Throughput

In the following we will show that although simple, NJNP can achieve a system throughput that is close to the optimal. Let us denote $\mathrm{E}[\mathcal{H}^*]$ as the optimal system throughput achievable with any online scheduling schemes.

First, we have the following theorem on $\mathcal{H}_{njnp}$ with light requests intensity, i.e., when the aggregated request arrival rate at the mobile charger $\lambda \to 0$.

Theorem 1. *In terms of the asymptotic system throughput, the performance of NJNP is within a constant factor of the optimal results when the requests intensity in the network is light. Specifically*

$$\frac{\mathrm{E}[\mathcal{H}_{njnp}]}{\mathrm{E}[\mathcal{H}^*]} \ge \frac{d_2 + vT_c}{d_1 + vT_c} \text{ as } \lambda \to 0,$$

where $d_1 \approx 0.52$ and $d_2 \approx 0.38$.

Proof. Clearly, comparing with the non-preemptive NJN discipline, NJNP further reduces the travel time to reach the target node. Thus the system throughput is also increased. Furthermore, the asymptotical service time with NJN is shown to be shorter than that with FCFS in [22], and thus we have the following relationship

$$\mathrm{E}[\mathcal{H}_{njnp}] \ge \mathrm{E}[\mathcal{H}_{njn}] \ge \mathrm{E}[\mathcal{H}_{fcfs}] = \frac{1}{d_1/v + T_c}, \tag{11}$$

where $d_1 \approx 0.52$ is the expected distance between two random locations in the system area, which can be obtained by (1).

When the charging request intensity in the system is light ($\lambda \to 0$), the asymptotically shortest travel distance for the mobile charger to reach the charging node is lower bounded by the expected distance between the field center and a random location in the network ((17) in [27]). Denote this distance as d', its distribution can be obtained by

$$f'_D(d') = \begin{cases} \pi d'^2 & 0 \le d' \le 1/2 \\ d'^2 \left(\pi - 4 \cos^{-1}\left(\frac{1}{2d'}\right) \right) & \\ \quad + 2d' \sin\left(\cos^{-1}\left(\frac{1}{2d'}\right) \right) & 1/2 < d' \le \sqrt{2}/2 \\ 0 & \text{otherwise} \end{cases},$$

where the first two cases are based on whether the random location falls in the inscribed circle of the square area. Similar results can be found in [28]. Denote $d_2 = E[d'] \approx 0.383$, then

$$\mathrm{E}[\mathcal{H}^*] \le \frac{1}{d_2/v + T_c}. \tag{12}$$

Theorem 1 follows by combining (11) and (12). ☐

Next we consider the scenario of heavy requests intensity in the network, namely, when $\lambda \to \frac{1}{T_c}$.

Theorem 2. *In terms of the asymptotic system throughput, the performance of NJNP is within a constant factor of the optimal results when the requests intensity in the network is heavy. Specifically*

$$\frac{\mathrm{E}[\mathcal{H}_{njnp}]}{\mathrm{E}[\mathcal{H}^*]} \ge \frac{d_4 + vT_c}{d_3 + vT_c} \text{ as } \lambda \to \frac{1}{T_c}.$$

where $d_3 \approx 0.64$ and $d_4 \approx 0.27$.

Theorem 2 can be proved based on (21) and (45) in [27]. We do not include the details here due to the space limit.

Theorem 1 and 2 reveal that when either the travel speed of the mobile charger is fast ($v \to \infty$) or the time to charge nodes is long ($T_c \to \infty$), the performance of NJNP approaches the optimal results. This is because the scheduling of the charging tasks only affects the charger travel distance, so when the time to charge a node is much longer than the charger travel time, all scheduling disciplines achieve comparable results.

3.2 Charging Latency with NJNP

3.2.1 Charging Latency Distribution

The most essential metric for nodes to evaluate the mobile charging process is the charging latency $\mathcal{R}$. For a given charging request arrives at the mobile charger at time t_0, let us denote the completion time of requests after its arrival as $\{t_1, t_2, ..., t_k\}$, where t_k is the completion time of this particular request. Then clearly, $t_k - t_0$ is the charging latency of this request, and asymptotically $(t_i - t_{i-1}) \sim f_{\mathcal{S}}(t) (1 \le i \le k)$. Thus by the convolution theorem, we have

$$\mathcal{R} = \sum_{i=1}^{k}(t_i - t_{i-1}) \sim f_{\mathcal{S}}^{(k)}(t), \qquad (13)$$

where $f^{(k)}(\cdot)$ is the k-fold convolution of $f(\cdot)$.

To further investigate the number of departures k, we again consider the scenario that l requests are waiting in the service pool. As discussed in (3), these l distances from the mobile charger to each of the requesting nodes can be viewed as l i.i.d. random variables, and thus asymptotically, the probability for any one of them to be the smallest is $\frac{1}{l}$. As a result, if the charger starts to charge a node during the next time slot, the probability for each of the l requesting nodes to be the charged node is also $\frac{1}{l}$. Thus k follows the distribution of

$$\Pr\{K = k\} = \left(1 - \sum_{l=1}^{N}\frac{\pi_l}{l(1 - \pi_0)}\right)^{k-1}\sum_{l=1}^{N}\frac{\pi_l}{l(1 - \pi_0)}, \quad (14)$$

where $\sum_{l=1}^{N}\frac{\pi_l}{l(1-\pi_0)}$ is the probability that a given request leaves the system each time when a departure occurs.

Combining (13) and (14), the charging latency conforms to

$$F_{\mathcal{R}}(t) = \sum_{k=1}^{N}\Pr\{K = k\}\int_{0}^{t}f_{\mathcal{S}}^{(k)}(x)dx. \qquad (15)$$

3.2.2 Optimality w.r.t. Charging Latency

Similar to the system throughput, we have the following two theorems on NJNP with respect to the charging latency under both light and heavy requests intensities[4]. Let $\mathcal{R}^*$

4. Note that we adopt a constant charging time in these theorems, which can be generalized for the case with heterogeneous charging time for sensor nodes. A potential approach is to update these theorems with the maximum charging time for the case of NJNP while adopting the minimum charging time for the optimal solution. In this way, it is still possible to obtain certain ratios between NJNP and the optimal solution to bound its optimality.

denote the minimal charging latency achievable for any online schedule schemes.

Theorem 3. *In terms of the asymptotic charging latency of requests, the performance of NJNP is within a constant factor of the optimal results when the requests intensity in the network is light. Specifically*

$$\frac{\mathrm{E}[\mathcal{R}_{njnp}]}{\mathrm{E}[\mathcal{R}^*]} \le \frac{d_1 + vT_c}{d_2 + vT_c} \text{ as } \lambda \to 0.$$

Proof. According to [22], $\mathcal{R}_{njn}$ is no longer than the response time for the FCFS discipline, or $\mathcal{R}_{fcfs}$. Thus, by Pollaczek-Khinchin (P-K) formula [21]

$$\mathrm{E}[\mathcal{R}_{njn}] \le \mathrm{E}[\mathcal{R}_{fcfs}] = \frac{\lambda(\frac{2E[d]T_c}{v} + E[(\frac{d}{v})^2])}{2(1 - \lambda d_1 - \lambda T_c)} + T_c + \frac{E[d]}{v},$$

(16)

where d is the distance between two random locations in the area as calculated by (1): $E[d] = d_1 \approx 0.52$.

A lower bound of $\mathrm{E}[\mathcal{R}^*]$ when the charging demands are light can be obtained with a similar idea as in [27],

$$\mathrm{E}[\mathcal{R}^*] \ge \frac{d_2}{v(1 - \lambda T_c)} + T_c \qquad (17)$$

The theorem follows by combining (16) and (17). □

Theorem 4. *In terms of the asymptotic charging latency of requests, the performance of NJNP is within a constant factor of the optimal results when the requests intensity in the network is heavy. Specifically*

$$\frac{\mathrm{E}[\mathcal{R}_{njnp}]}{\mathrm{E}[\mathcal{R}^*]} \le \left(\frac{d_3}{d_4}\right)^2 \text{ as } \lambda \to \frac{1}{T_c}.$$

Proof. According to [27], an upper bound of $\mathrm{E}[\mathcal{R}_{njn}]$ with heavy traffic is

$$\mathrm{E}[\mathcal{R}_{njn}] \le \frac{d_3^2 \lambda}{v^2(1 - \lambda T_c)^2} \text{ as } \lambda \to \frac{1}{T_c}. \qquad (18)$$

Furthermore, by considering the stable condition of the system and adopting the Little's law, we have

$$\mathrm{E}[\mathcal{R}^*] \ge \frac{d_4^2 \lambda}{v^2(1 - \lambda T_c)^2} - \frac{1 - 2\lambda T_c}{2\lambda}. \qquad (19)$$

The theorem follows from (18) and (19). □

Essentially, when the requests intensity is heavy, d_3 and d_4 correspond to the longest distance the mobile charger has to travel to charge a node with NJNP and the shortest distance the mobile charger has to travel in the optimal case, respectively. These travel distances have a twofold effect on the charging latency: on the time to serve one request and on the number of requests in the pool. This explains the quadric form of the constant in the theorem.

3.3 Fairness and Potential Starvation Issue

Similar to the traditional *Shortest-Seek-Time-First* (SSTF) discipline in disk scheduling and the *Shortest-Job-First* in CPU

scheduling [29], the gain of NJNP is achieved by sacrificing the faraway requesting nodes. However, counter-intuitively, it is shown in [30], [31] that NJNP-like greedy schemes can reduce the delay of at least 99 percent of clients, when compared with the fair sharing discipline. Furthermore, we argue that the unfairness with NJNP would be much less significant, which can be explained by the following reasons.

First, the distance between the charger and requesting nodes cannot be arbitrarily large, and is upper bounded by the longest distance in the field, i.e., $\sqrt{2}$ in a unit square sensing field. This indicates the requests service time is upper bounded as well. Second, the distance between the charger and a specific requesting node changes as the charger travels in the field, and the probability that it keeps at a large value during a long time period is small. These arguments can be verified by the charging latency distribution, as will be explained in Section 5.

To further alleviate the potential starvation issue, we propose a guideline on the proper setting of the remaining energy level of sensor nodes below which the charging requests will be sent out, such that there will be enough time for the charger to accomplish the charging tasks before starvation occurs, as will be explained in Section 4.2.

Further modifications can be applied to NJNP to address the unfairness issue when necessary. One possible approach is to assign certain sequence properties among the sensor nodes, and the charger carries out the mobile charging process by combining the NJNP discipline with these nodes sequences. We have explored the charging scheduling design along this direction in our recent work [32].

4 GUIDANCES ON NJNP IMPLEMENTATION

The analytical results on NJNP not only reveal insights on the on-demand charging process, but also guide its practical implementations. We in this section use two examples to show how the analytical results can assist the implementation of NJNP in practice.

4.1 Network Scenario

For clarity, we first present the system scenario in a more quantitive manner. Consider a sensor network with N nodes deployed in a unique square area. The energy capacity of each node is C_s, and nodes can actively estimate their energy consumption rate r_e. When the residual energy is below $\theta_e C_s (0 < \theta_e < 1)$, the node will send a charging request to the mobile charger. The mobile charger travels at speed v and serves the received requests with NJNP. The energy capacity of the mobile charger is C_m, which can be replenished at the energy tank at the center of the area. The energy consumption for the charger to travel one meter is e_t, and the charging efficiency is $\eta (0 < \eta \le 1)$. The request *missing ratio*, defined as the probability that nodes fail to be charged before energy depletion, is required to be no larger than θ_p.

4.2 Determining θ_e

The remaining energy level θ_e plays a critical role in the charging process. If the charging request is sent too early (with a too large θ_e), it is very likely that when the mobile charger arrives at the target node, the node still has a sufficient energy supply. This not only degrades the efficiency of the mobile charger but also increases the charging latency for other requesting nodes. On the other hand, if the node sends the charging request too late (with a too small θ_e), the time left for the charger to travel to and charge the node is limited, which increases the requests missing ratio.

In the following, we demonstrate how our analytical results on the charging latency distribution can guide the setting of a proper θ_e. In stable systems with a large number of nodes, the fact that a specific node is waiting to be charged has a negligible effect on the aggregated request arrival rate at the mobile charger. Thus, the following relationship between the aggregated request arrival rate λ and the energy level θ_e exists

$$\lambda \approx \frac{r_e N}{(1 - \theta_e)C_s}, \tag{20}$$

where $(1 - \theta_e)C_s$ is the energy that a fully charged node can use before sending out its charging request. Based on the charging latency distribution with NJNP, we can set the optimal θ_e under the maximal tolerable charging missing ratio θ_p by following a *fixed-point iteration* approach. Start with $\theta_e = 0$ and calculate the corresponding estimated $\hat{\theta}_p$ according to the latency distribution shown in (15). If $\hat{\theta}_p > \theta_p$, then increase θ_e with a small step length Δ. Repeat the process until we find the smallest θ_e satisfying the requirement on $\hat{\theta}_p$. Obviously, more efficient method such as binary search could be adopted to further accelerate the calculation. The algorithm returns a proper θ_e if feasible solution exists, otherwise (if returns $\theta_e = 1$) we need to either increase the nodes energy capacity or the required θ_p.

Homogeneous energy consumption rates of all nodes are assumed in the above example. In a more general case with heterogeneous energy consumption rates, it is also possible to find θ_e^i for each node i by modifying (20) accordingly.

4.3 Determining C_m

The energy capacity C_m of the mobile charger also has a significant impact on the charging process. A too small capacity severely restricts the mobile charger's ability to continuously provide the charging service to devices, while a too large energy capacity is also undesirable, due to both the diminishing returns in reducing the charging latency of devices and the increase in both the size and weight of energy storage device.

Obviously, it is undesirable if the mobile charger has to return to the energy tank for energy replenishment while pending requests still exist in its service pool. Denote this event as $\mathbb{A}$. Thus the energy capacity of the mobile charger should be at least large enough to guarantee that $\mathbb{A}$ occurs only with a very small probability.

The probability for event $\mathbb{A}$ to occur is highly related to the busy period of the mobile charger, defined as the time from a request enters an empty service pool of the mobile charger until the pool becomes empty again. Thus we characterize the distribution of the mobile charger's busy period first.

Clearly, the busy period is the sum of the service times of several successively served requests. Then if we can obtain

the distribution of the number of served requests in a given busy period, denoted as Y, we can adopt the convolution theorem to derive the distribution of the busy period.

Denote $b_i^j (1 \leq i \leq j)$ as the probability that starting with i requests in the service pool, at most j requests are served before the pool becomes empty again. Clearly, $b_1^1 = a_0^1$, as defined in (7). When considering $b_i^j (j > 1)$, we can see that at most $j - i$ new arrivals can occur during the period. If $k(1 \leq k \leq j - i)$ requests arrive during the service of the first request, the departure of the first request will leave behind a service pool of size $i + k - 1$. Also note that at most $j - 1$ departures can occur after the departure of the first request, which happens with probability b_{i+k-1}^{j-1}. Combining the case with $j = 0$, we have the following linear relationships among b_i^j:

$$b_i^j = \begin{cases} a_0^1 + \sum_{k=1}^{j-1} a_k^i b_k^{j-1} & i = 1 \\ a_0^i x_{i-1}^{j-1} + \sum_{k=1}^{j-i} a_k^i b_{i+k-1}^{j-1} & 2 \leq i \leq j - 1 .. \\ a_0^j b_{i-1}^{j-1} & i = j \end{cases}$$

By summing over all the possible numbers of arrivals during the service of the first request, the distribution of Y can be calculated as:

$$\Pr\{Y \leq y\} = a_0^1 + \sum_{j=1}^{y-1} a_j^1 b_j^{y-1},$$

and $\Pr\{Y = y\}$ can be calculated accordingly. Then based on (8) and (13), the busy period distribution of the mobile charger can be calculated as:

$$F_{\mathcal{B}}(t) = \sum_{y=1}^{N} \Pr\{Y = y\} \int_0^t f_{\mathcal{S}}^{(y)}(x) dx.$$

The energy required for the mobile charger to *survive* a busy period consists of two parts: for the mobile charger to continuously stay in service throughout this busy period, and for the mobile charger to return to the energy tank for energy replenishment afterwards when necessary. We investigate these two parts respectively.

The energy consumption of the mobile charger to charge individual devices comes from two aspects: to travel to the devices and to charge them. For a given busy period with length t, assume the mobile charger charges y devices during this period. Clearly, $1 \leq y \leq \lfloor \frac{t}{T_c} \rfloor$. Given an energy volume x_1, let us define a binary function $u(x_1, t, y)$ as:

$$u(x_1, t, y) = \begin{cases} 1 & x_1 \geq e_t v(t - y T_c) + \frac{y C_s}{\eta} \\ 0 & \text{otherwise} \end{cases} .$$

Then the energy required for the mobile charger to continuously stay in service throughout this busy period follows the following distribution:

$$F_{e_1}(x_1) = \int_0^\infty f_{\mathcal{B}}(t) \sum_{y=1}^{\lfloor t/T_c \rfloor} \Pr\{Y = y\} u(x_1, t, y) dt.$$

The energy consumed by the mobile charger to return to the energy tank, denoted as x_2, depends only on the travel distance of the mobile charger, which follows the

distribution of:

$$f_{e_2}(x_2) = \frac{1}{e_t} f_{D'}\left(\frac{x_2}{e_t}\right),$$

where $f_{D'}(\cdot)$ is the distribution of the distance from the energy tank to a random location in the network as in (12).

Thus the energy required for the mobile charger to *survive* a busy period follows the distribution of

$$f_e(x) \sim f_{e_1}(x_1) * f_{e_2}(x_2). \tag{21}$$

Based on (21), we can find the minimal energy capacity C_m for the mobile charger such that $\int_0^{C_m} f_e(x) > 1 - p_A$, where p_A is the maximal tolerable probability for event $\mathbb{A}$ to occur.

5 EVALUATIONS

The evaluations of our work consist of three parts. We first validate the soundness of the queue-based system modeling, and then we numerically evaluate the analysis of the NJNP-based mobile charging process. Finally, more insights on the impacts of different network parameters are revealed with an event-driven simulator.

5.1 Model Verification

Our analysis on NJNP is based on the $M/G/1/NJNP$ queuing model. Thus before evaluating the analysis accuracy, we first verify the soundness of the model. Specifically, we verify the assumption on the Poisson arrival of charging requests to the mobile charger, which means their inter-arrival time is exponentially distributed.

We verify the Poisson arrival by simulating an event-driven network in a field of size 100×100 m^2, and the charger travel speed is 1 m/s based on the parameters from real-world robots [3]. When an event occurs at a random location in the area, nodes within a distance of 10m can detect it, and the corresponding information is generated and forwarded to the control center through multi-hop communications. Nodes have a full energy capacity of $C_s = 100$. Two cases of the transmission/reception energy costs of $e_{tx} = e_{rx} = 0.02$ and $e_{tx} = e_{rx} = 0.05$ per packet are explored, respectively. Nodes send out charging requests when their remaining energy is below a pre-defined threshold $0.044 C_s$ (this value is set according to the guidance on determining θ_e introduced in Section 4.2, and will be explained in details in Section 5.2.3). The charger serves these requests and fully charges nodes according to NJNP. We record the request arrival time at the charger, calculate their inter-arrival times, and compare them with two exponential distributions with the same mean values.

The verification results are shown in Fig. 5, where the average of the inter-arrival time with $e_{tx} = e_{rx} = 0.02$ is around 250 s, indicating an arrival rate λ at the mobile charger of roughly 0.004, and those for $e_{tx} = e_{rx} = 0.05$ are around 100 s and 0.01, respectively. The consistence between exponential distributions and simulation results indicates our model is sound.

The Poisson arrival is further verified by the Kolmogorov-Smirnov (K-S) test [33] with a significance level of 0.05. With a total number of 50×2 tests on the request inter-arrival times obtained with 50 different topologies, only 1 of them
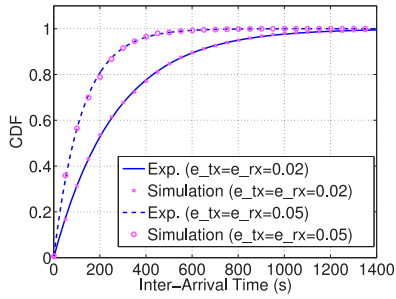
Fig. 5. Verify Poisson arrival.

TABLE 1
Correlation Between the l Distances

l	2	3	4	5	6
Max	0.0219	0.0299	0.0199	0.0186	0.0177
Mean	0.0087	0.0097	0.0057	0.0071	0.0080

with $e_{tx} = e_{rx} = 0.02$ rejects the hypotheses that the inter-arrival time is exponentially distributed, and all those with $e_{tx} = e_{rx} = 0.05$ are accepted.

To validate the independence among charging requests, we have recorded the service time of individual charging requests during the simulated mobile charging process, and adopt the 1-lag autocorrelation as the metric to statistically evaluate their correlations. Based on the results obtained with 100 network topologies, the maximum and minimum of the absolute values of the correlation are 0.18995 and 0.00005, respectively, with an average of 0.05708, and their CDF is shown in Fig. 6. These small correlation values validate the independence among charging requests and thus further validate our queue-based modeling.

5.2 Numerical Evaluation

In the numerical evaluation, we generate a Poisson requests arrival sequence in the temporal dimension with given intensity λ, and these requests are randomly assigned to the sensor nodes to give each request a spatial property (i.e., the location of the corresponding sensor node). Then the mobile charger carries out the charging process according to the proposed NJNP scheme.

5.2.1 System Throughput

Two cases of the node-level request arrival rates, i.e., the frequency for individual nodes to send out its charging request, are explored with $\lambda' = 0.00005$ and $\lambda' = 0.00025$, indicating an average node lifetime of about $\frac{1}{0.00005} s \approx 5.5$h and $\frac{1}{0.00025} s \approx 1.1$ h, respectively. These node-level arrival rates are chosen according to the empirical results from [1]: an ultra-capacitor with a capacitance of 22 F indicates a typical lifetime of around 2.15 h for MicaZ motes at 10 percent duty cycle. With a total number of 100 nodes, these roughly correspond to request arrival rates at the mobile charger of 0.005 and 0.025, respectively.
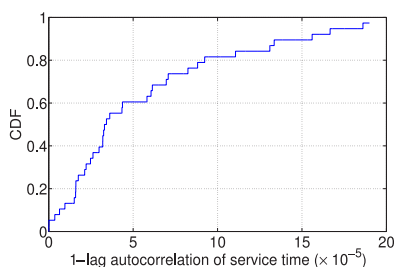
The analysis on the shortest distance from requesting nodes to the mobile charger is based on the first-order statistic, which requires all these variables are i.i.d. We run the simulation with a given location of the mobile charger and l requesting nodes, and calculate these l distances. We repeat this calculation for $10,000$ times with different value of $l = 2, 3, \ldots, 6$, and calculate the pairwise correlation coefficients of these l distance sequences. The maximal and mean correlation of the $\frac{l(l-1)}{2}$ sequence pairs are shown in Table 1. The small correlation supports our methodology.

The verification results on the probability that a service is preempted are shown in Fig. 7, where the x-axis is the distance between the mobile charger and the selected target node, and y-axis is the probability that this charging request is preempted before the mobile charger reaches the node. Our analytical results can capture the preemption probability reasonably well. The increase of the preemption probability with the initial distance is intuitive, because the longer travel time offers more chances for the preemption to happen. Furthermore, the verification results indicate that our results are actually a lower bound of the preemption probability. This is because our analysis is based on a continuous distance distribution $F_D(d)$, which suggests every location in the area should be occupied by a node. As a result, a term of $1 - q_d(j)$ for every possible j is included in (4). However, not all of these $1 - q_d(j)$ need to be considered in practice, because there may not exist a node of distance $d - jv\delta_t$ to the current location of the charger.

Fig. 8 shows the evaluation results on the system throughput (i.e., the number of charging requests that the charger accomplished in a unit time), where the time to fully charge an energy-depleted node T_c is 10s. The match between the analysis and simulation results indicates a good accuracy of our analysis. Furthermore, the throughput increases as the requests intensity becomes heavier, which can be explained by two reasons. First, a higher demands intensity leads to a larger number of requests in the service pool, and thus makes it more likely for the mobile charger to select a closer target node. This in turn increases the system throughput. Second, from (4), it is clear that a larger

Fig. 6. Correlation of requests.
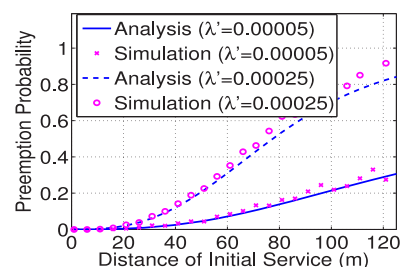
Fig. 7. Preemption probability.
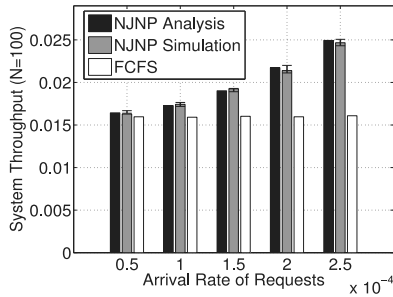
Fig. 8. System throughput with 100 nodes.
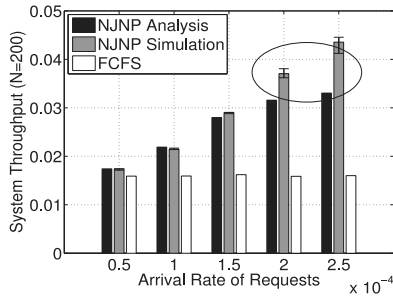
Fig. 9. System throughput with 200 nodes.
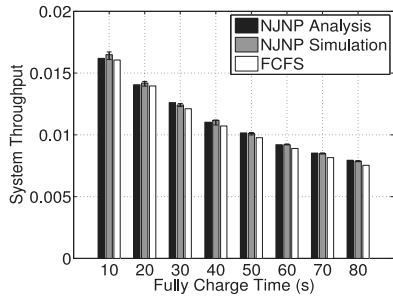
Fig. 10. System throughput with $T_c(\lambda' = 0.00005)$.

Fig. 11. System throughput with $T_c(\lambda' = 0.00025)$.
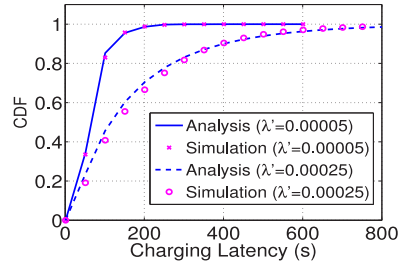
Fig. 12. Charging latency with 100 nodes.
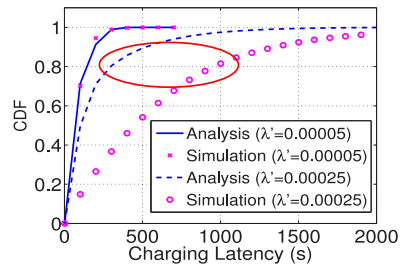
Fig. 13. Charging latency with 200 nodes.

request arrival rate increases the preemption probability, which reduces the service time and thus increases the system throughput as well. The system throughput under FCFS with identical settings are shown for comparison. A clear advantage of NJNP over FCFS can be observed, especially when the requests arrival rates are high. This is because more pending requests make it more likely for NJNP to find closer nodes to charge.

A well-known condition for stable queuing systems is that the system utilization ratio ρ should be smaller than 1. This implies that for our analysis to hold, the condition that $\lambda'NE[\mathcal{H}_{njnp}] < 1$ must be guaranteed. To verify this, we increase the number of nodes to 200 and repeat the simulation. The results are shown in Fig. 9. We can see that our analysis is still accurate when λ' is relatively small, e.g., below 1.5×10^{-4} in Fig. 9. However, the deviation between the analysis and simulation results increases quickly when λ' increases from 1.5×10^{-4}, because the stable condition of the system does not hold anymore.

To investigate the effect of T_c on the charging process, we record the system throughput when T_c varies from 10 to 80 s. The results with the node-level request arrival rates of 0.00005 and 0.00025 are shown in Figs. 10 and 11, respectively. The match between the analysis and simulation results when $\lambda' = 0.00005$ verifies the accuracy of our analysis.

However, when λ' is 0.00025, our analysis tends to underestimate the system throughput when T_c is large. This is again due to the invalidation of the stable system condition. Note that the advantage of NJNP over FCFS is not so obvious in Fig. 10, because with such a light requests intensity, the number of requests in the service pool is limited, which offers little chances for the greedy feature of NJNP to take effect.

5.2.2 Charging Latency

Fig. 12 shows the evaluation results on the charging latency distribution with $N = 100$. The match of the analysis and simulation results not only verifies our results, but also indicates that the proposed guidance on determining the optimal node remaining energy level should perform well, as we will see in Section 5.2.3. The charging latency distribution with $N = 200$ is shown in Fig. 13. The results with $\lambda' = 0.00005$ are still accurate. However, due to the invalidation of the stable condition, our analysis deviates from the simulation when $\lambda' = 0.00025$. Furthermore, we can see the tail of the charging latency distribution is not excessively long, especially when compared with the typical lifetime of nodes, i.e., $20,000$ and $4,000$s with λ' of 0.00005 and 0.00025, respectively. This observation indicates the unfairness issue with NJNP is not severe. To gain a more clear view on the unfairness issue, Table 2 presents the ratios of missed requests from the three disciplines with a maximal tolerable charging latency of 400 s. We can see that NJNP achieves the smallest miss ratio with all λ', which means the charging service

TABLE 2
Miss Ratio of Requests

λ'	0.00005	0.0001	0.00015	0.0002	0.00025
FCFS	0.0001	0.0152	0.3141	0.9823	0.9997
NJN	0.0001	0.0028	0.0181	0.0564	0.1216
NJNP	0.0001	0.0025	0.0139	0.0467	0.1050

provided by the mobile charger is the most reliable with NJNP. Note that when $\lambda' = 0.0002$ and $\lambda' = 0.00025$, the miss ratio with FCFS almost reaches 1 due to an unstable system.

5.2.3 Effectiveness of System Design Guidances

We investigate the effectiveness of the proposed guidance on the implementation of NJNP in the next.

- *Determining* θ_e. We consider an energy capacity $C_s = 100$, and the long-term energy consumption rate is $r_e = 0.01$, which indicates a node lifetime of around $\frac{100}{0.01}$ s ≈ 1.5 h. We require that $\hat{\theta}_p < \theta_p = 0.01$. We run the simulation with different remaining energy levels, and record the resultant $\hat{\theta}_p$. Then we use the guidance presented in Section 4.2 to estimate the optimal value of θ_e. The simulation results and the optimal setting returned by the proposed guidance are shown in Fig. 14. We can see the θ_e returned by the proposed guidance satisfies our requirement pretty well: it has to be as small as possible while guaranteeing $\hat{\theta}_p < 0.01$. The returned θ_e (4.4 percent of the full energy capacity of nodes) is adopted in the simulation when verifying the arrivals, as mentioned in Section 5.1.

- *Determining* C_m. The effectiveness of the proposed method to guide the selection of the energy capacity of the mobile charger is verified in Fig. 15. The request arrival rate is 0.01, the energy cost for the mobile charger to travel one meter is $e_t = 0.05$, the energy capacity $C_s = 100$, and the charging efficiency is $\eta = 0.5$. We run the simulation with different energy capacities for the mobile charger and record the probability of nodes failed to be charged before energy depletion. Then we calculate the smallest energy capacity of the mobile charger that guarantees it can survive the busy periods in 99.99 percent of the time based on (21). The results show that the proposed method performs well in determining a proper C_m, and further increases the mobile charger's energy capacity only gains little in terms of reducing the missing ratio of charging requests.

5.3 Event-Driven Simulation

An event-driven simulator is built to further evaluate the NJNP-based mobile charging process. We simulate a camera sensor network with 50–500 randomly deployed nodes. The sensing field size is $100 \text{ m} \times 100 \text{ m}$, and a sink is located at
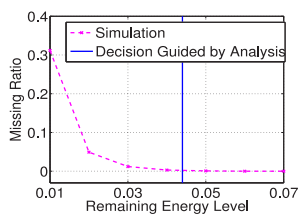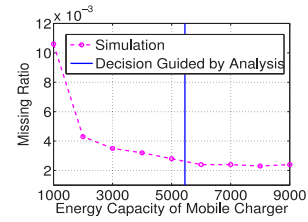
Fig. 15. Determine C_m.

the field center. The current draw to capture a single photo is 600 mA, which is typical for camera sensors [34]. The communication energy costs of sensor nodes are set based on the data sheet of MICA2 node: with transmitting and receiving current draw of 25 and 8 mA, respectively. After the deployment of sensor nodes, a routing structure is constructed based on the TinyOS standard CTP [35]. Then the environment information, after being captured by individual nodes, is transmitted to the sink through multi-hop communications based on the routing structure. The energy capacity of fully charged sensor nodes is $1,000 \text{ mAh}$. Sensor nodes send out charging requests to the charger when their remaining energy is below 4.4 percent of its total energy supply, which is set according to the guidance on determining θ_e introduced in Section 4.2. The charger serves these requests and fully charges nodes according to NJNP, with a travel speed of 1 m/s [3]. We simulate a network operation period of $500,000 \text{ s}$ in each simulation, and the reported results in the following are averaged with 100 simulation runs.

5.3.1 Variance of Node Energy Consumptions

The perfect estimation on the node energy consumption is challenging in practice because nodes may have various energy consumptions over time. We in the next explore how the variance on node energy consumptions affects the NJNP-based mobile charging process.

Fig. 16 shows the charging latency of sensor nodes during the simulated mobile charging process with different levels of node energy consumption variance. We can see that the charging latency increases as the variance becomes larger, especially for the worst-case charging latency (i.e., the top of these bars). This is because a larger variance in node energy consumptions makes the unfairness issue among sensor nodes more significant, which may significantly prolong the charging latency of certain nodes. However, we can see the average charging latency increases much slower when compared with the worst-case charging latency. This indicates that NJNP shows a

Fig. 14. Determine θ_e.
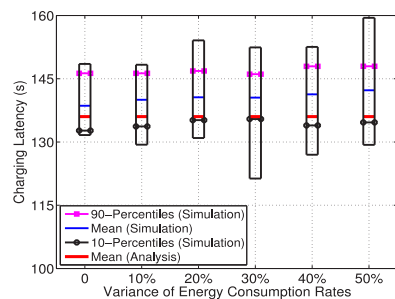
Fig. 16. Charging latency with energy consumption variance.
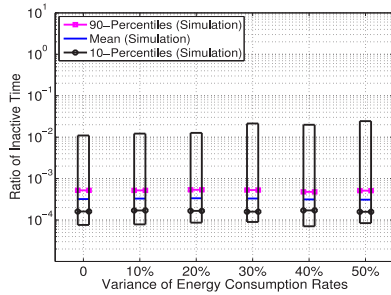
Fig. 17. Inactive time ratio with energy consumption variance.

Fig. 19. Inactive time ratio with delivery failure ratio of charging requests.

good tolerance on the dynamic node energy consumptions in most cases. Furthermore, comparing the average charging latency obtained through simulation and analysis, we can see although the gap between them becomes wider with a larger variance, the deviation is still kept below 10 s even with a variance as large as 50 percent, indicating a good robustness of the analysis over the variance in node energy consumptions.

Requesting sensor nodes may deplete their energy supply and are forced into the inactive state if the mobile charger fails to respond to their charging requests (i.e., charge the nodes) on time. Fig. 17 shows the inactive time ratio of sensor nodes with varying energy consumption variance. The small inactive time ratio (typically between 10^{-4} to 10^{-2}) indicates a good sustainable operation of sensor nodes. Furthermore, we can see the average of inactive time ratio is quite stable with regard to the node energy consumption variance, which again indicates that the node energy consumption variance has a quite limited impact on the charging process.

5.3.2   Failure Probability in Requests Delivery

The charging requests of sensor nodes need to be sent to the mobile charger through wireless communications, which may be lost due to the dynamic network conditions. We in the next investigate the impact of potential delivery failures of charging requests on the mobile charging process. Specifically, sensor nodes wait for a timer of 10 s to expire before re-requesting if the delivery of the current request is failed. The charging latency and the inactive time ratio obtained with varying requests delivery failure probabilities are shown in Figs. 18 and 19, respectively.

Intuitively, the charging latency increases as the delivery failure probability becomes larger, as observed from Fig. 18. Furthermore, compared with the case of 0 failure probability, the average charging latency is only increased by about
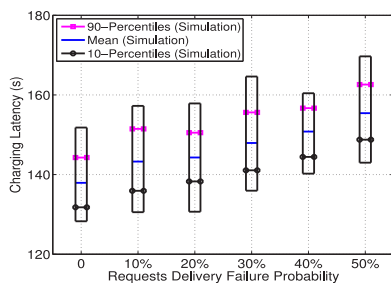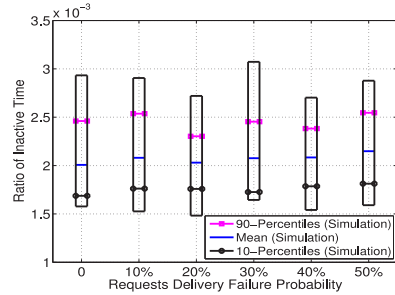
$\frac{155-138}{138} = 12.3$ percent with a delivery failure probability as high as 50 percent. Similar observations can be obtained from Fig. 19 on the inactive time ratio of sensor nodes. We can see the increasing trend of inactive time ratio is even more mild when compared with that of the charging latency, because a longer charging latency may but will not always lead to the energy depletion of nodes. These observations demonstrate that NJNP has a good tolerance on the request delivery failures.

5.3.3   Network Densities

The charging latency and inactive time ratio obtained with a varying number of sensor nodes in the network are shown in Figs. 20 and 21, respectively. We can see both the latency and inactive time ratio increases with a larger network scale due to a heavier workload at the mobile charger. However, the increasing speed is mild when the number of nodes is below 200, but it increases dramatically when further increasing the nodes number. This is because the charger workload becomes too heavy in this case, which violates the stability condition of the queuing model (i.e., $\rho < 1$). Employing multiple mobile chargers to collaboratively carry out the charging process is a potential approach to address this issue. Note that with the proposed $M/G/1/NJNP$ queuing model, we can effectively identify such critical charger workload levels, and thus determine whether multiple mobile chargers are required for the application under consideration.

6   PRACTICAL ISSUES

6.1   Non-Poisson Arrival

Our queue-based modeling and analysis are based on the assumption of the Poisson arrival of requests. This greatly simplifies our analysis with the memoryless property of the inter-arrival time of requests, while at the same time

Fig. 18. Charging latency with delivery failure ratio of charging requests.
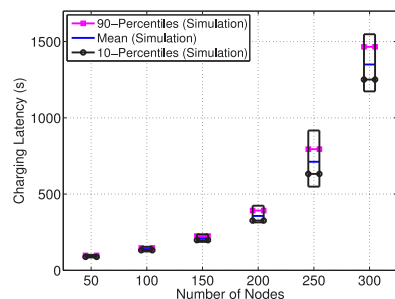
Fig. 20. Charging latency with the number of nodes.
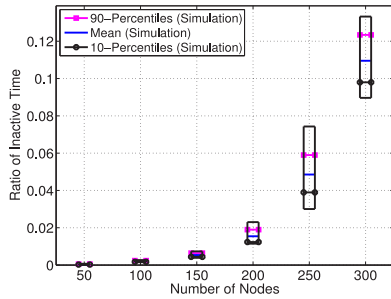
Fig. 21. Inactive time ratio with the number of nodes.

Fig. 22. State transition diagram with general arrivals.

captures the reality reasonably well, as verified in Section 5. However, if in some cases the Poisson arrival fails to capture the actual situation in a reasonably sound way, we need to consider the problem with a general arrival process.

Carefully examining the analysis on the $M/G/1/NJNP$ queuing model, we can observe that the only part that strictly requires a Poisson arrival is (7), or the number of new arrivals during a service, denoted as X for simplicity. Thus if we are able to characterize X with a general arrival process, the analysis can be carried out with the same approach. However, the computation complexity is likely to be much higher in this non-Poisson case, because with the memoryless property of Poisson arrival, X is only determined by the arrival rate and the length of the service time, while in a more general case, we need to consider the start time of the service. Denote $p_{i,j}$ as the probability that a new arrival from sensor node $j(j = 1, 2, ..., N)$ occurs during the service selected from i waiting requests. We discretize the probability interval $[0, 1]$ into m slots according to the accuracy requirements, i.e., $p_{i,j}$ can only take a value from $\{\frac{1}{m}, \frac{2}{m}, \ldots, 1\}$. Thus for each i, there are m^N combinations of the probability $p_{i,j}$ for each node, and we need to consider X with each of these combinations. In this way, the system states can be represented by the tuple of $\{i, Z_{i,j}\} = \{i, < p_{i,1}, p_{i,2}, \ldots, p_{i,N} >_j\}(j = 1, 2, \ldots, m^N)$, and the state transition chain will become two dimensional, as shown in Fig. 22. Clearly, both the number of states and the possible transitions of the chain are of the order $O(N \cdot m^N)$, compared with an order of $O(N)$ with Poisson arrival.

The above analysis is on the case that we have no knowledge on the arrival process. It is possible in most of the cases to find certain pattern of the arrival process, based on the specific application under consideration. This observed pattern can help to reduce the complexity of the chain, in terms of both the number of states and the number of possible transitions. For example, if the energy consumption rates of sensor nodes are relatively stable, the arrival process of charging demands will show strong periodic feature. Thus, some states in the chain will only occur with a negligible probability. Furthermore, for a given sensor node, the probability for it to send a charging request in the near future does not change arbitrarily between consecutive time slots, which means the number of possible transitions in the chain can also be reduced.

6.2 Analytical Framework for DMC Problem

Although we focus on the specific charging scheme NJNP in this paper, the queue-based modeling approach can serve as
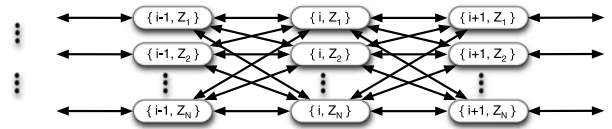
a modularized and generalized analytical framework, and can be applied to many different on-demand mobile charging scenarios. The most critical component in the framework is the time for the charger to accomplish one charging task, i.e., the service time of the queuing system. In practice, the service time consists of three parts: 1) the request delivery time defined as the time since a sensor node sends out its charging request to the time the request is received by the charger, 2) the travel time for the mobile charger to travel to the requesting sensor node, and 3) the charging time for the charger to accomplish the charging of the requesting node. We assume a negligible request delivery time and a worst-case charging time is this paper. Even when the request delivery time is not negligible or when the charging time needs to be considered in detail, we can still use the convolution theorem to derive the service time distribution based on the distributions of the three components. After characterizing the service time, the analysis can be carried out with a general approach according to the queuing model.

7 RELATED WORK

A number of research works have been devoted to adopting nodes with controlled mobility to accomplish the data collection in wireless sensor networks [3], [4], [22]. Although introducing mobility is shown to be able to improve the system performance, only a few work is done on utilizing the controlled mobility to replenish the energy supply of individual nodes [9], [10].

On the other hand, replenishing node energy by harvesting energy from surrounding environment has been extensively studied [36], [37]. Many of these studies observed that the harvested energy is unevenly distributed among nodes [38], and how to use the concept of energy sharing to improve the node lifetime has attracted more and more attention [2]. An obvious difference between these works with ours is the lack of controlled mobility in consideration.

For those limited works that exploited mobility to accomplish the energy replenishment of the nodes in sensor networks, most of them focused on the offline scenario [5], [6], which is quite different from the DMC problem in our consideration, in terms of the application scenarios, problem settings, and research objectives.

To the best of our knowledge, the most closely related works are [9], [10], where the mobile charger shares its limited energy supply with individual nodes through wireless recharging in a dynamic network environment. On top of these state-of-the-art designs, we aim to establish a theoretical foundation on the DMC problem, which serves as a good benchmark for the evaluation of more advanced scheme design.

NJNP is similar to the preemptive version of the *Shortest-Seek-Time-First* discipline in disk scheduling [29]. However, the diversity with SSTF resides in a one-dimensional space,

i.e., the tracks of the disk, while that of NJNP is in a two-dimensional space, i.e., the field. Clearly, this difference makes the analysis on NJNP more challenging. The DMC problem investigated in this paper is similar to the dynamic scheduling problems such as *dynamic vehicle routing* [39] and *dynamic traveling salesman problem* [40], [41]. Greedy schemes similar to the non-preemptive version of NJNP have been explored in [42], [43], and our analysis advances the investigation by incorporating the preemption and obtaining the probability distributions of critical performance metrics.

8 CONCLUSIONS

In this paper, we have analytically evaluated the on-demand mobile charging problem under the discipline of NJNP. Analytical results on the system throughput and charging latency have been presented and their closeness to the optimal solutions have been proved. Furthermore, we have demonstrated two examples on how to use the analysis to guide the implementation of NJNP in practice. The accuracy of the analytical results and the efficiency of the proposed system design guidances have been verified through extensive simulations.

REFERENCES

[1] T. Zhu, Z. Zhong, Y. Gu, T. He, and Z.-L. Zhang, "Leakage-aware energy synchronization for wireless sensor networks," in *Proc. 7th Int. Conf. Mobile Syst., Appl., Serv.*, 2009, pp. 319–332.
[2] T. Zhu, Y. Gu, T. He, and Z. Zhang, "eShare: A capacitor-driven energy storage and sharing network for long-term operation," in *Proc. 8th ACM Conf. Embedded Netw. Sensor Syst.*, 2010, pp. 239–252.
[3] G. Xing, T. Wang, W. Jia, and M. Li, "Rendezvous design algorithms for wireless sensor networks with a mobile base station," in *Proc. 9th ACM Int. Symp. Mobile Ad Hoc Netw. Comput.*, 2008, pp. 231–240.
[4] J. Luo and J. Huabux, "Joint sink mobility and routing to maximize the lifetime of wireless sensor networks: the case of constrained mobility," *Trans. Netw.*, vol. 18, no. 3, pp. 871–884, 2010.
[5] Y. Shi, L. Xie, Y. T. Hou, and H. D. Sherali, "On renewable sensor networks with wireless energy transfer," in *Proc. INFOCOM*, 2011, pp. 1350–1358.
[6] S. Zhang, J. Wu, and S. Lu, "Collaborative mobile charging for sensor networks," in *Proc. IEEE 9th Int. Conf. Mobile Ad-Hoc Sensor Syst.*, 2012, pp. 84–92.
[7] L. Fu, P. Cheng, Y. Gu, J. Chen, and T. He, "Minimizing charging delay in wireless rechargeable sensor networks," in *Proc. INFOCOM*, 2013, pp. 2922–2930.
[8] S. Guo, C. Wang, and Y. Yuan, "Mobile data gathering with wireless energy replenishment in rechargeable sensor networks," in *Proc. INFOCOM*, 2013, pp. 1932–1940.
[9] Y. Peng, Z. Li, W. Zhang, and D. Qiao, "Prolonging sensor network lifetime through wireless charging," in *Proc. 31st IEEE Real-Time Syst. Symp.*, 2010, pp. 129–139.
[10] Z. Li, Y. Peng, W. Zhang, and D. Qiao, "J-RoC: A joint routing and charging scheme to prolong sensor network lifetime," in *Proc. 19th IEEE Int. Conf. Netw. Protocols*, 2011, pp. 373–382.
[11] L. Xie, Y. Shi, Y. T. Hou, W. Lou, H. D. Sherali, and S. F. Midkiff, "On renewable sensor networks with wireless energy transfer: the multi-node case," in *Proc. 9th Annu. IEEE Commun. Soc. Conf. Sensor, Mesh Ad Hoc Commun. Netw.*, 2012, pp. 10–18.
[12] L. Xie, Y. Shi, Y. T. Hou, W. Lou, and H. D. Serali, "On traveling path and related problems for a mobile station in a rechargeable sensor network," in *Proc. 14th ACM Int. Symp. Mobile Ad Hoc Netw. Comput.*, 2013, pp. 109–118.
[13] (2014). Supercapacitors. [Online]. Available: http://batteryuniversity.com
[14] (2014). Powercast. [Online]. Available: http://www.powercastco.com/
[15] (2014). WISP. [Online]. Available: http://www.seattle.intel-research.net/WISP/
[16] A. Noda and H. Shinoda, "óSelective wireless power transmission through high-Q ßat waveguide-ring resonator on 2-D waveguide sheet," *IEEE Trans. Microw. Theory Tech.*, vol. 59, no. 8, pp. 2158–2167, Aug. 2011.
[17] M. C. Silverman, D. Nies, B. Jung, and G. S. Sukhatme, "Staying alive: A docking station for autonomous robot recharging," in *Proc. IEEE Int. Conf. Robot. Autom.*, 2002, pp. 1050–1055.
[18] (2014). Roomba. [Online]. Available: http://www.irobot.com/
[19] (2014). "Nokia Wireless Charging Plate. [Online]. Available: http://www.nokia.com/global/products/accessory/dt-900/
[20] V. Kulathumani, A. Arora, M. Sridharan, and M. Demirbas, "Trail: A distance-sensitive sensor network service for distributed object tracking," *ACM Trans. Sens. Netw.*, vol. 5, no. 2, pp. 1–40, 2009.
[21] D. Gross, *Fundamentals of Queueing Theory*, 4th ed. New Jersey, NY, USA: Wiley, p. 232, 2008.
[22] L. He, Z. Yang, J. Pan, L. Cai, and J. Xu, "Evaluating service disciplines for mobile elements in wireless ad hoc sensor networks," in *Proc. INFOCOM*, 2012, pp. 576–584.
[23] M. Ahmadi and J. Pan, "Random distances associated with trapezoids," *arXiv:1307.1444*, 2013.
[24] H. A. David and H. N. Nagaraja, *Order Statistics*, 3rd ed. New Jersey, NJ, USA: Wiley, 2003.
[25] S. L. Albin, "On Poisson approximations for superposition arrival processes in queues," *Manage. Sci.*, vol. 28, no. 2, pp. 126–137, Feb. 1982.
[26] C. Y. T. Lam and J. P. Lehoczky, "Superposition of renewal processes," *Adv. Appl. Probability*, vol. 23, no. 1, pp. 64–85, 1991.
[27] J. Bertsimas and G. V. Ryzins, "A stochastic and dynamic vehicle routing problem in the Euclidean plane," *Oper. Res.*, vol. 39, pp. 601–615, 1991.
[28] R. Larson and A. Odoni, *Urban Operations Research.* Englewood Cliffs, NJ, USA: Prentice Hall, 1981.
[29] Silberschatz and Galvin, *Operating System Principles*, 7th ed. New York, NY, USA: Wileys.
[30] N. Bansal and M. Harchol-Balter, "Analysis of SRPT scheduling: Investigating unfairness," in *Proc. Int. Conf. Meas. Modeling Comput. Syst.*, 2001, pp. 279–290.
[31] C. Hong, M. Caesar, and P. Godfrey, "Finishing flows quickly with preemptive scheduling," in *Proc. Conf. Appl., Technol., Archit. Protocols Comput. Commun.*, 2012, pp. 127–138.
[32] L. He, L. Fu, L. Zheng, Y. Gu, P. Cheng, J. Chen, and J. Pan, "Esync: An energy synchronized charging protocol for rechargeable wireless sensor networks," in *Proc. 15th ACM Int. Symp. Mobile Ad Hoc Netw. Comput.*, 2014, pp. 247–256.
[33] (2014). K-S test. [Online]. Available: http://www.physics.csbsju.edu/stats/KS-test.html
[34] P. Kulkarni, D. Ganesan, P. Shenoy, and Q. Lu, "SensEye: A multi-tier camera sensor network," in *Proc. 13th Annu. ACM Int. Conf. Multimedia*, 2005, pp. 229–238.
[35] O. Gnawali, R. Fonseca, K. Jamieson, D. Moss, and P. Levis, "Collection tree protocol," in *Proc. 7th ACM Conf. Embedded Netw. Sensor Syst.*, 2009, pp. 1–14.
[36] M. Gorlatova, P. Kinget, I. Kymissis, D. Rubenstein, X. Wang, and G. Zussman, "Challenge: Ultra-low-power energy-harvesting active networked tags (EnHANTs)," in *Proc. 15th Annu. Int. Conf. Mobile Comput. Netw.*, 2009, pp. 253–260.
[37] A. Kansal, J. Hsu, S. Zahedi, and M. Srivastava,, "Power management in energy harvesting sensor networks," *ACM Trans Embedded Comput. Syst.*, vol. 6, no. 4, pp. 1–37, 2007.

[38] J. Taneja, R. Katz, and D. Culler, "Defining CPS challenges in a sustainable grid," in *Proc. IEEE/ACM 3rd Int. Conf. Cyber-Phys. Syst.*, 2012, pp. 119–128.

[39] S. L. Smith, M. Pavone, F. Bullo, and E. Frazzoli, "Dynamic vehicle routing with heterogeneous demands," in *Proc. 47th IEEE Conf. Decision Control*, 2008, pp. 1206–1211.

[40] G. Ghiani, A. Quaranta, and C. Triki, "New policies for the dynamic traveling salesman problem," *Optim. Methods Softw.*, vol. 22, no. 6, pp. 971–983, 2007.

[41] G. D. Celik and E. H. Modiano, "Controlled mobility in stochastic and dynamic wireless networks," *Queueing Syst.*, vol. 72, no. 3–4, pp. 251–277, 2012.

[42] E. Altman and H. Levy, "Queueing in space," *Adv. Appl. Probability*, vol. 26, no. 4, pp. 1095–1116, 1994.

[43] D. J. Bertsimas and G. V. Ryzin, "A stochastic and dynamic vehicle routing problem in the euclidean plane," *Oper. Res.*, vol. 39, no. 4, pp. 601–615, 1991.
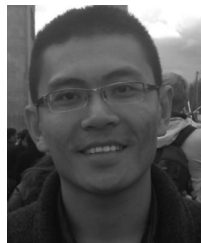
Liang He (S'09-M'12) received the BEng degree in 2006 and the PhD degree in 2011 from Tianjin University, China, and Nankai University, China, respectively. He is currently a research fellow at The University of Michigan at Ann Arbor, MI, USA. Before joining UMich, he worked as a research scientist at the Singapore University of Technology and Design from 2011 to 2014. From October 2009 to October 2011, he worked at the University of Victoria as a research assistant. He has been a recipient of the best paper awards of QShine'14, IEEE WCSP'11, and IEEE GLOBECOM'11. He is a member of the IEEE and ACM.

Linghe Kong (S'09-M'13) received the Dipl. Ing. degree in telecommunication from TELECOM SudParis in 2007, the BE degree in automation from Xidian University in 2005, and the PhD degree in computer science from Shanghai Jiao Tong University in 2012. He is currently a post-doctoral researcher in Shanghai Jiao Tong University and McGill University. He also worked as a postdoctoral researcher at the Singapore University of Technology and Design from 2013 to 2014. His research interests include wireless sensor networks and mobile computing. He is a member of the IEEE.

Yu (Jason) Gu received the PhD degree in the Department of Computer Science and Engineering from the University of Minnesota, 2010. He is currently a research scientist at IBM Research, Austin. He was an assistant professor at the Singapore University of Technology and Design from 2010 to 2014. He is the author and co-author of more than 90 papers in premier journals and conferences. His publications have been selected as a graduate course materials by more than 10 universities in the United States and other countries. He has received several prestigious awards from the University of Minnesota. He is a member of the IEEE.
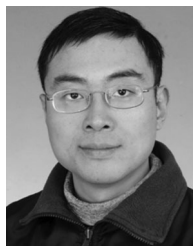
Jianping Pan (S'96-M'98-SM'08) received the bachelor's and PhD degrees in computer science from Southeast University, Nanjing, Jiangsu, China, and did his postdoctoral research at the University of Waterloo, Waterloo, Ontario, Canada. He is currently an associate professor of computer science at the University of Victoria, Victoria, British Columbia, Canada. He also worked at Fujitsu Labs and NTT Labs. His area of specialization is computer networks and distributed systems, and his current research interests include protocols for advanced networking, performance analysis of networked systems, and applied network security. He received the IEICE Best Paper Award in 2009, the Telecommunications Advancement Foundation's Telesys Award in 2010, the WCSP 2011 Best Paper Award, the IEEE Globecom 2011 Best Paper Award, the JSPS Invitation Fellowship in 2012, and the IEEE ICC 2013 Best Paper Award, and has been serving on the technical program committees of major computer communications and networking conferences including IEEE INFO-COM, ICC, Globecom, WCNC and CCNC. He is the Ad Hoc and Senor Networking Symposium co-chair of IEEE Globecom 2012 and an associate editor of the *IEEE Transactions on Vehicular Technology*. He is a senior member of the ACM and the IEEE.
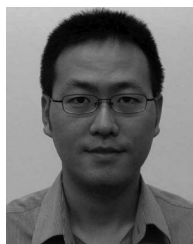
Ting Zhu received the BS and ME degrees from the Department of Information Science and Electronic Engineering at the Zhejiang University in 2001 and 2004, respectively, and the PhD degree from the Department of Computer Science and Engineering at the University of Minnesota in 2010. He is now an assistant professor in the Department of Computer Science and Electrical Engineering at the University of Maryland, Baltimore County. He was an assistant professor at the State University of New York, Binghamton, from 2011 to 2014. His research interests include wireless networks, renewable energy, embedded systems, distributed systems, and security. He is a member of the IEEE.

▷ **For more information on this or any other computing topic, please visit our Digital Library at** www.computer.org/publications/dlib.